



# Replacement of the part of gravity model and of remaining dynamic models by empirical accelerations in the fit processes of a low-Earth satellite orbit and factors limiting their accuracy

Andrzej Bobojć<sup>1</sup>

Received: 14 March 2023 / Accepted: 1 September 2023 / Published online: 7 October 2023  
© The Author(s) 2023

## Abstract

This work contains the results of calculations performed to prove the ability of estimated orbital parameters for the replacement of dynamic models in the orbit determination of a sample low-Earth-orbiting satellite. The obtained solutions include two cases of the absorption of dynamic models. In the first case, the contribution of dynamic models, apart from the gravity field, was absorbed, i.e., the satellite motion was described by the gravity field and estimated parameters. In the second case, the contributions of all dynamic models, including the gravity field, were absorbed. For the gravity field model, the absorption concerned its selected parts. In this case, the satellite motion was modeled only by the gravity model truncated to different degrees and orders and an appropriate set of orbital parameters. In both aforementioned cases, the initial conditions were also improved. Cartesian coordinates of the Gravity Field and Steady-State Ocean Circulation Explorer Mission satellite along selected reference arcs of the official reduced-dynamic orbit served as pseudo-observations in this study. The orbital parameters, also known as empirical accelerations, were determined using the least-squares method by a dedicated orbital package. The results were presented and compared in the form of the root-mean-square (RMS) values of the differences between the estimated orbits and the reference orbits, as well as the corresponding values of the obtained empirical accelerations for selected variants of solutions. The obtained accuracy of the process of the fit of the satellite orbit expressed by the corresponding RMS values, reached a millimeter level. For selected typical solutions, the distribution of residuals and power spectra are presented with an indication of characteristic errors: random and systematic periodic components. Key factors influencing the obtained fit accuracies of estimated orbits are given. Contributions of these factors in the error budget of fits of estimated orbits are also presented. Additionally, in the fit process, the performance of selected gravity models coming from different years is compared to assess the impact of gravity field errors on the results of aforementioned process.

**Keywords** Empirical accelerations · Satellite orbit estimation · Dynamic models · Gravity field models

## Introduction

One of the key factors determining the fulfillment of goals of various space missions is the knowledge of orbits of satellites associated with them. The accuracy of determining these orbits depends on the accuracy of observations, usually made using an onboard Global Navigation Satellite

System receiver, and on the accuracy of models describing the gravitational and non-gravitational perturbing forces acting on a satellite. Thus, an increase in the accuracy of the determination of orbits can be achieved by improving an observation base and measurement techniques in conjunction with the development of observation processing methods and by improving dynamic models. These models include the gravity field model and other models generating satellite accelerations due to, *inter alia*, the solid Earth tides, the ocean tides, the attraction of the Sun, Moon and planets, the relativistic effects, the atmospheric drag and the direct and reflected solar radiation pressure. The mentioned improvement of the dynamic models (in this case, the direct and reflected radiation pressure models) was carried out, for example, by Mao et al. (2021) in

---

Edited by Prof. Maria Marsella (ASSOCIATE EDITOR) / Prof. Ramon Zuñiga (CO-EDITOR-IN-CHIEF).

✉ Andrzej Bobojć  
altair@uwm.edu.pl

<sup>1</sup> Department of Geodesy, University of Warmia and Mazury in Olsztyn, Olsztyn, Poland

the process of determining the orbits of such satellites as Sentinel 3A, Sentinel 3B and Swarm-C. Additionally, in order to reduce existing deficiencies of the used dynamic models, the estimation of empirical parameters was also applied (Mao et al. 2021). A similar strategy consisting of limiting the inaccuracies of the dynamic models by estimating empirical parameters was used in determining the orbits of satellites, for example, for such missions as the Challenging Mini-Satellite Payload (Reigber et al. 2005), the Gravity Recovery and Climate Experiment (GRACE) (Kang et al. 2003; Tapley et al. 2004), for the altimetric satellites ENVISAT and GFO (Moore and Wang 2005), for the Gravity Field and Steady-State Ocean Circulation Explorer mission (GOCE) (Rummel et al. 2011) and the Gravity Recovery and the Climate Experiment Follow-On mission (Kang et al. 2020). The orbits obtained in this way are characterized by a reduced impact of dynamic models (Jäggi et al. 2006). However, it was not only the inaccuracies of dynamic models that were subject to partial compensation by estimating empirical accelerations. For example, in (Wang et al. 2022), the authors determine the real-time orbits of GRACE satellites, omitting modeling perturbations caused by the ocean tides, the relativistic effects and the Earth's radiation pressure. These perturbations were absorbed by the corresponding empirical accelerations.

The available official orbit of a low-Earth-orbiting satellite from the aforementioned GOCE mission (Bock et al. 2011) is a reference for the numerical experiments carried out in this work on further increasing the impact of empirical parameters on estimated orbits by the partial and the total absorption of the contribution of the gravity field model and contributions of other dynamic models, respectively. The motivation to undertake this research was the following question: Can the use of only the gravity field (without or with truncation) and empirical parameters to provide sufficient accuracy of obtained orbits? In other words, will the estimated sets of empirical parameters allow sufficient absorption for the contribution of dynamic models? Or are the empirical parameters "capacious" enough to absorb the partial contribution of the gravity field and the entire contribution of the remaining dynamic models, maintaining a similar level of accuracy as in the case when these models are used? To answer these questions, various solutions of the fit of satellite orbit to the official orbit were obtained, where the Cartesian coordinates of the satellite positions in this orbit were treated as pseudo-observations. The results obtained by (Jäggi et al. 2007) are an additional promising motivation to conduct the research in the described aspect. In the cited work, the orbits of GRACE A and B satellites were determined based on undifferenced and doubly differenced Global Positioning System measurements using only the EIGEN-CG03C gravity model and a set of estimated

empirical parameters, dominated by pseudo-stochastic parameters determined in 6-min intervals. The accuracy of the obtained orbits after validation with the Satellite Laser Ranging technique was at the centimeter level (Jäggi et al. 2007).

The first part of the work (Sects. "Methodology", "Solutions for the absorption of the contribution of the remaining dynamic models", "Solutions for the absorption of part of the gravity model and of the remaining dynamic models") contains a description of the research, and the results in terms of the root-mean-square (RMS) of fitting the estimated orbital arcs to the official orbit using only the gravity field with sets of empirical parameters and the truncated gravity field with the corresponding empirical accelerations. Also, the RMS values of estimated empirical accelerations for particular orbital arcs without the use of dynamic models are given and compared to the corresponding values for the case of the use of dynamic models in the orbit determination process. In the second part of the work (Sect. "Analysis of the accuracy of the obtained results" and its Sects. "Fit accuracy analysis: distance residuals in the time domain and in the frequency domain", "Fit accuracy analysis: estimating the effect of random errors of the reference orbit on the fit of selected arcs", "Fit accuracy analysis: estimating the impact of random errors of the gravity model on the fit of selected arcs"), an analysis of the obtained fit accuracy is performed. In the frame of this analysis, the residuals of orbit determination process as the distances of the estimated orbits from the reference orbit at successive epochs and the corresponding power spectra are presented for the selected solutions. Next, the impacts of a few factors on the results of orbit fits are quantitatively estimated. These factors include errors of the reference orbit, discretization errors related to the algorithm of the orbit determination process and errors of the gravity field model. The final Sect. "Summary and conclusions" provides the summary and conclusions.

## Methodology

The following equation can be written to describe the satellite motion in reference to the problem studied in this work:

$$\ddot{\mathbf{r}}(t) = \ddot{\mathbf{r}}_G(t) + \ddot{\mathbf{r}}_{\text{RPF}}(t). \quad (1)$$

In this vector Eq. (1), the satellite accelerations are represented as second-order time derivatives of the satellite position vector  $\mathbf{r}$  in the inertial frame. The vector  $\ddot{\mathbf{r}}(t)$  is the total acceleration of the satellite, while the vectors  $\ddot{\mathbf{r}}_G(t)$  and  $\ddot{\mathbf{r}}_{\text{RPF}}(t)$  are accelerations generated by the static part of the gravity field and remaining perturbing forces at the epoch  $t$ , respectively. The components of the first term  $\ddot{\mathbf{r}}_G(t)$  on the right-hand side of Eq. (1) are spatial

derivatives of the geopotential. The second term  $\ddot{\mathbf{r}}_{\text{RPF}}(t)$  is generated by gravitational and non-gravitational perturbing forces. Both vectors  $\ddot{\mathbf{r}}_{\text{G}}(t)$  and  $\ddot{\mathbf{r}}_{\text{RPF}}(t)$  are generated by the dynamic models, i.e., by the gravity model and by the remaining models describing the aforementioned perturbing forces, respectively.

In this work, the vector  $\ddot{\mathbf{r}}_{\text{G}}(t)$  is either not replaced or is partially replaced by additionally estimated empirical accelerations. Partial replacement means using the truncated gravity model. In the case of the vector  $\ddot{\mathbf{r}}_{\text{RPF}}(t)$ , a complete absorption takes place by estimating the aforementioned accelerations. Thus, the contribution of the remaining dynamic models is expressed by a set of empirical parameters.

For the adopted satellite, these models include the solid Earth tides, the ocean tides, the attraction of the Sun, Moon, planets and solar radiation pressure. This satellite, with an exceptionally low orbit with an average altitude of about 250 km, was the main component of the aforementioned gravity field study mission GOCE (Bock et al. 2011, 2014; Drinkwater et al. 2003).

Sets of corrections to the satellite initial state vector (initial conditions) and empirical parameters in the form of accelerations were determined using the following observation equation:

$$\mathbf{r}^o(t) + \mathbf{v}(t) = \mathbf{r}^c(t) + \sum_{i=1}^6 \frac{\partial \mathbf{r}^c(t)}{\partial p_i} (p_i - p_{i0}) + \sum_{i=1}^N \frac{\partial \mathbf{r}^c(t)}{\partial \mathbf{a}_i} (\mathbf{a}_i - \mathbf{a}_{i0}). \quad (2)$$

The quantities  $\mathbf{r}^o(t)$  and  $\mathbf{r}^c(t)$  are the observed and computed position vectors in a given epoch  $t$ , respectively. The positions of the adopted satellite expressed by the components of the vector  $\mathbf{r}^o(t)$ , i.e., the Cartesian coordinates  $x^o(t)$ ,  $y^o(t)$ ,  $z^o(t)$  delivered by the European Space Agency, were the observations in the process of fitting the satellite orbit. In turn, the vector  $\mathbf{v}(t)$  is the vector of residuals in the epoch  $t$ . Next,  $p_i$  ( $i = 1, 2, \dots, 6$ ) are the estimated corrections to the initial conditions and  $\mathbf{a}_i$  ( $i = 1, 2, \dots, N$ ) are the vectors of estimated empirical accelerations. The a priori values of estimated parameters are denoted by  $p_{i0}$ ,  $\mathbf{a}_{i0}$ . An important part of the observation Eq. (2) are the partial derivatives  $\partial \mathbf{r}^c(t) / \partial p_i$  and  $\partial \mathbf{r}^c(t) / \partial \mathbf{a}_i$  of the computed position vector  $\mathbf{r}^c(t)$  with respect to the corresponding parameters in a given epoch  $t$ . In order to perform an orbit determination process, these derivatives were propagated to subsequent epochs by the numerical integration of an appropriate variational equation.

As already mentioned, the estimated parameters were in the form of accelerations, which were determined as constant values in the subsequent equal time intervals. Hence, the determined orbital arcs were divided into the mentioned equal time intervals. Moreover, in each interval, three parameters were determined, whose absolute values

are equal to the lengths of acceleration vectors in three constant directions relative to the position of the satellite in an osculating orbit. The first direction coincides with the instantaneous velocity vector of the satellite, i.e., this is the tangent direction, the second direction coincides with the instantaneous radial vector of the satellite; in other words, it is the radial direction with an orientation from the Earth's center of mass to the satellite. Finally, the third direction, called the normal direction, is perpendicular to the plane of the osculating orbit and coincides with the vector that forms a right-handed frame with the vectors defining the other two directions. The satellite acceleration vectors in the three mentioned directions in successive epochs (with respect to the inertial frame) are determined using the estimated acceleration parameters in these directions multiplied by the corresponding directional cosines. Thus, the resultant vector of empirical acceleration in a given epoch is the sum of these three determined vectors in the aforementioned directions expressed in the inertial frame. The Eq. (1) in relation to the estimation of empirical parameters can thus be written as:

$$\ddot{\mathbf{r}}(t) = \ddot{\mathbf{r}}_{\text{G-ntr/tr}}(t) + \ddot{\mathbf{r}}_{\text{emp}}(t). \quad (3)$$

In this equation, the total epoch-wise satellite acceleration  $\ddot{\mathbf{r}}(t)$  is approximated by the sum of the acceleration  $\ddot{\mathbf{r}}_{\text{G-ntr/tr}}(t)$  derived from the non-truncated or truncated gravity field and the estimated empirical acceleration  $\ddot{\mathbf{r}}_{\text{emp}}(t)$ , which absorbs the perturbing acceleration resulting from the remaining dynamic models.

A basic tool in this work was a dedicated package, which was presented in Drozyner (1995). In order to adapt this package to the specifics of the analyzed problem, additional procedures for the estimation of empirical accelerations were added and implemented. The key feature of the used software is the ability to perform the satellite orbit improvement using a set of taken observations by the estimation of the corrections to the components of the initial state vector and aforementioned empirical parameters in the frame of the least-squares approach. The initial state vectors for estimated arcs were taken from the corresponding arcs of the reference orbit for the first epochs. When improving the orbit, its propagation is realized by the numerical integration of the equations of motion using Cowell's eighth-order algorithm. All calculations were performed with respect to the aforementioned inertial frame, whose definition can be found, for example, in ESA (2010). The data acquired for this work through the European Space Agency, in addition to the mentioned Cartesian coordinates of the official reduced-dynamic GOCE orbit, also include elements of the transformation from the International Terrestrial Reference Frame 2005 to the inertial frame.

As a result of the performed numerical tests, two basic groups of solutions were obtained for the aforementioned options without the absorption of the gravity model, with the partial absorption of this model and with the full absorption (for both cases) of the contribution of the remaining dynamic models. To emphasize the efficiency of the estimated empirical accelerations, additional solutions were also determined without the replacement of the contribution of dynamic models. In this case, for the adopted satellite, apart from the gravity model, models generating accelerations from the solid Earth and ocean tides, the attraction of the Sun, Moon and planets, the relativistic effects and the pressure of direct and reflected solar radiation were also included. A detailed description of these models can be found in (Bobojć and Drożyner 2011).

A quality indicator of the solutions used in this work is a kind of the root-mean-square of the difference between the estimated orbit and the corresponding official GOCE orbit (reference orbit). This indicator was determined according to the following formula:

$$\text{RMS}_{3D} = \sqrt{\sum_{i=1}^3 (\text{RMS}_i)^2}. \quad (4)$$

The lower subscript 3D shows the dependence of the indicator  $\text{RMS}_{3D}$  on the  $\text{RMS}_i$  ( $i = 1, 2, 3$ ) values, which are the RMS differences of the corresponding Cartesian coordinates on the determined orbit and on the reference orbit.

### Solutions for the absorption of the contribution of the remaining dynamic models

In Table 1, the  $\text{RMS}_{3D}$  values for estimated orbital arcs are presented. These arcs are the 90-min and 1-day arcs for selected initial epochs in 2009 and 2010. For the given satellite, the 90-min arc reflects approximately one of its orbital revolutions while the 1-day arc contains about 16 such revolutions. The gravity model Tongji-Grace02k (Chen et al. 2018) up to the degree and order of 180 was used in the calculations. The remaining effects affecting the satellite motion are modeled by the estimated accelerations in the three directions specified above. In this case, 269 and 1,500 empirical accelerations in equal time intervals were estimated in each of the three directions for the 90-min and 1-day arcs, respectively. As shown in Table 1, the obtained fits of the estimated orbital arcs remain at the level of a few millimeters. In view of the accuracy of the official GOCE orbit at 2 cm (Bock et al. 2014), these values may be considered in the numerical sense.

**Table 1** Solutions of the orbit determination process in terms of the fit of the estimated 90-min and 1-day arcs to the satellite's official orbit. Motion modeling: the gravity model and the set of empirical accelerations

Arc number	DOY <sup>a</sup>	90-min arcs (mm)	1-day arcs (mm)	1-day arcs (mm <sup>b</sup> )
#1	311 2009	1.7	2.3	7.5/3.3 <sup>c</sup>
#2	324 2009	2.8	3.3	10.3/3.1
#3	334 2009	2.8	3.3	10.1/3.1
#4	337 2009	2.8	3.3	10.1/3.1
#5	353 2009	1.7	2.3	7.3/3.2
#6	364 2009	1.7	2.3	7.3/3.2
#7	7 2010	1.7	2.3	7.5/3.3
#8	14 2010	3	3.5	8.7/2.5
#9	17 2010	1.7	2.3	7.4/3.2
#10	25 2010	3	3.5	8.8/2.5

<sup>a</sup>Day of year

<sup>b</sup>Maximal distance between the estimated and the reference arc for the 1-day arcs,

<sup>c</sup> $M_D$  to  $\text{RMS}_{3D}$  ratio for the 1-day arcs

Table 1 shows that the fit for the individual arcs is in the range from 1.7 to 3.0 mm (90-min arcs) and in the range from 2.3 to 3.5 mm (1-day arcs). The change of the gravity model to the ITG-Grace2010s (Mayer-Gürr et al. 2010) model, under the same numerical conditions, did not change the  $\text{RMS}_{3D}$  value for the particular 1-day arcs with an accuracy of 0.1 mm. This may be due to the similarity of both models obtained on the basis of data from the GRACE mission. The results in Table 1 (at the level of a few millimeters) show for both arc lengths differences of about one millimeter. The arcs #1, #5, #6, #7, #9 differ from the other five arcs by a better fit slightly above 1 mm. The differences in the  $\text{RMS}_{3D}$  values for the obtained arcs may reflect differences in the accuracy of corresponding reference arcs. On the other hand, the same level of fit for the given arcs as discussed above was also achieved if the remaining dynamic models were also included in the process of determining the orbit (these results are not shown here). Comparing the results for the two arc lengths considered, one can see the clear systematic decrease in the fit accuracy when going from the 90-min arcs to the 1-day arcs. This decrease in all cases ranges from 0.5 to 0.6 mm. It indicates the accumulation of estimation errors with increasing arc length. Considering all the obtained  $\text{RMS}_{3D}$  values for both arc lengths, it can be seen that the estimated arcs can be divided into three groups depending on the accuracy of the fit. The first group, with the highest accuracy, includes the arcs #1, #5, #6, #7 and #9, the second group, with significantly lower accuracy, is formed by the arcs #2, #3, #4, while the third group consists

of the arcs #8 and #10 with slightly lower accuracy than the arcs of the second group.

The last column of Table 1 contains values for the maximum distances of the estimated 1-day orbits from the 1-day reference orbits. These values, labeled  $M_D$ , range from 7.3 to 10.1 mm. They clearly show their relationship to the  $RMS_{3D}$  values. In general, larger the  $RMS_{3D}$  values correspond to larger the  $M_D$  values. The exceptions are the arcs #8 and #10 ( $RMS_{3D} = 3.5$  mm), which have smaller the  $M_D$  values (about 9 mm) compared to the arcs #2, #3, #4 ( $RMS_{3D} = 3.3$  mm), which show an increase in  $M_D$  to a level of about 10 mm. In the case of the factor characterizing the value of  $M_D$  versus  $RMS_{3D}$ , one can see a clear decrease in its value as the accuracy of the fit decreases (increasing  $RMS_{3D}$ ). For the most accurate arcs #1, #5, #6, #7, #9  $M_D$  is greater than  $RMS_{3D}$  from 3.2 to 3.3 times, for the arcs #2, #3, #4 of the intermediate accuracy the considered factor decreases to 3.1, and for the arcs #8, #10 of the lowest accuracy a decrease to the smallest value of 2.5 is visible.

The same number of estimated empirical accelerations for both variants—with and without using the remaining dynamic models resulted in a corresponding change in their value. To illustrate this, Table 2 shows the increase in the RMS value of the sets of estimated accelerations ( $RMS_a$ ), going from the case of using the remaining dynamic models to the case of excluding them in the fit process. In this case, the gravity model ITG-Grace2010s was used and the same number of estimated parameters as for the results in Table 1 was taken. The results for the five selected orbital arcs are given. First of all, it is worth noting here the clear relationship between the  $RMS_{3D}$  values for particular arcs and the  $RMS_a$  values of the estimated empirical accelerations. More specifically, for the same number of estimated empirical accelerations, the worse fit (larger  $RMS_{3D}$ ) corresponds to a smaller level of values of these accelerations (smaller  $RMS_a$ ). It is as if the

**Table 2** Increase of  $RMS_a$  values of the estimated acceleration sets for the selected 1-day arcs with and without using the remaining dynamic models. The case: 1500 estimated accelerations per each of the three directions

Arc number	$RMS_{3D}$ (mm)	${}^aRMS_a$ (m/ $s^2$ )	${}^bRMS_a$ (m/ $s^2$ )	Increase in $RMS_a$ value (%)
#1	2.3	$2.42 \times 10^{-6}$	$2.49 \times 10^{-6}$	2.9
#2	3.3	$1.46 \times 10^{-6}$	$1.53 \times 10^{-6}$	4.8
#3	3.3	$1.46 \times 10^{-6}$	$1.57 \times 10^{-6}$	7.5
#8	3.5	$8.20 \times 10^{-7}$	$9.18 \times 10^{-7}$	12
#10	3.5	$8.43 \times 10^{-7}$	$1.02 \times 10^{-6}$	21

<sup>a</sup>Values for the solutions with the use of the remaining dynamic models

<sup>b</sup>Values for the solutions without the use of the remaining dynamic models

empirical accelerations were subject to some kind of limitation in the estimation process under less favorable numerical conditions, e.g., with slightly larger random errors of the reference orbit. Table 2 shows that the obtained  $RMS_a$  values are in the order of  $10^{-6}$  m/s<sup>2</sup>. The larger  $RMS_a$  acceleration values occur for solutions without the remaining dynamic models (fourth column of Table 2) because, in this case, the differences between the orbit determined before the application of estimated accelerations (only the initial condition improvement) and the reference orbit are, on average, over three times greater for solutions without the remaining dynamic models than for the corresponding solutions (also only the initial condition improvement) using these models. Hence, the need to reduce for a larger spatial distance between the orbits is related to the estimation of accelerations with larger  $RMS_a$  values. The increase in the  $RMS_a$  acceleration values for the variants of solutions without the use of remaining dynamic models compared to the variants using these models ranges from 2.9 to 21.0% (Table 2).

## Solutions for the absorption of part of the gravity model and of the remaining dynamic models

In the following computation variants, the gravity model Tongji-Grace02k was truncated to selected degrees and orders of the spherical harmonic coefficients without taking into account the remaining dynamic models. In other words, the satellite motion was determined by the truncated gravity model, improved initial conditions, and the set of empirical accelerations. The fit of estimated arcs at the millimeter level was obtained by improving the initial conditions and determining the appropriate acceleration sets of estimated parameters for each solution.

Table 3 includes the results for the short arc with a length close to 90 min, which corresponds to the one revolution of the satellite. This arc is the initial part of the 1-day arc #1 (2009 DOY 311). Table 3 clearly shows the efficiency of empirical accelerations, where despite the successive truncating of the gravity model, the fit is maintained at a level of about 1.7 mm up to the degree and order of  $2 \times 0$  of the gravity field, which corresponds to the gravity field up to the  $C_{20}$  coefficient. After omitting it there is a clear deterioration of the fit to the value of about 2.9 mm (Table 3) for the main Newtonian term in the field  $0 \times 0$  (only the  $C_{00}$  coefficient). This means a degradation in the fit of about 1 mm. The similar pattern of keeping the same level of fit up to the field  $2 \times 0$  and about the 1-mm loss of accuracy, was observed for the other nine 90-min arcs, obtained as the initial parts of the 1-day arcs listed in Table 1. Theoretically, one would expect a continuous increase in the RMS of the estimated accelerations as the range of the omitted coefficients of the

**Table 3** Fits of the selected short 90-min arc for the different degree and order of the gravity model truncation without using the remaining dynamic models. The case: 269 estimated accelerations per each of the three directions

Truncation to degree and order	RMS <sub>3D</sub> (mm)	RMS <sub>a</sub> (m/s <sup>2</sup> )
180×180 <sup>a</sup>	1.7	1.75×10 <sup>-5</sup>
160×160	1.7	1.75×10 <sup>-5</sup>
140×140	1.7	1.75×10 <sup>-5</sup>
120×120	1.7	1.75×10 <sup>-5</sup>
100×100	1.7	1.75×10 <sup>-5</sup>
80×80	1.7	1.76×10 <sup>-5</sup>
60×60	1.7	1.82×10 <sup>-5</sup>
40×40	1.7	2.08×10 <sup>-5</sup>
20×20	1.7	3.58×10 <sup>-5</sup>
10×10	1.7	5.21×10 <sup>-5</sup>
5×5	1.7	8.63×10 <sup>-5</sup>
2×2	1.7	1.25×10 <sup>-4</sup>
2×0	1.7	1.40×10 <sup>-4</sup>
0×0	2.9	1.06×10 <sup>-2</sup>

<sup>a</sup>No truncation—the full gravity field model

gravity field model increases. This increase is indeed visible; however, only from the truncation of the gravity field model up to the degree and order of 80 (Table 3). In other words, the same level of empirical accelerations of  $1.75 \times 10^{-5}$  m/s<sup>2</sup>, with the same fitting accuracy of 1.7 mm, occurs for both the starting case, i.e., without truncation—the model up to degree and order of 180, as well as for subsequent variants of truncation up to degree and order of 100. These results show that gravity field coefficients from degree and order of 180 to degree and order to 100 do not have a significant impact on the satellite orbit determination. Thus, it can also be stated that the orbit of given satellite is sensitive to the gravity field coefficients up to the degree and order of less than 100, when estimating empirical accelerations as the set of piecewise constant accelerations. A more detailed investigation of this case showed that an increase in the RMS of the estimated accelerations occurs for truncation of the gravity model up to degree and order of 81. Thus, for this 90-minute short arc, a significant component of the gravity model reaches degree and order of 81 of the spherical harmonics coefficients. Similar studies conducted for another 90-min arc (the initial part of arc #10-2010 DOY 25) showed an even smaller significant component of the gravity model—namely up to the degree and order of 77 of the spherical harmonics coefficients.

For the longer 1-day arcs, the efficiency of empirical accelerations in terms of truncating the gravity field Tongji-Grace02k up to the degree and order of 2, was also checked. The same arcs and the same number of estimated accelerations were assumed as for the tests presented in

**Table 4** Results of the fit of the estimated 1-day arcs to the corresponding reference arcs for the gravity field truncation up to degree and order of 2 and the omission of the remaining dynamic models. Numbers of estimated accelerations: (a) 1500 per direction (b) 2000 per direction

Arc number	DOY	(a) RMS <sub>3D</sub> (mm)	(b) RMS <sub>3D</sub> (mm)
#1	311 2009	4.3	2.7 <sup>c</sup> /2.3 <sup>d</sup>
#2	324 2009	5	3.6/3.3
#3	334 2009	4.9	3.6/3.3
#4	337 2009	4.8	3.5/3.3
#5	353 2009	4.3	2.7/2.3
#6	364 2009	4.3	2.7/2.3
#7	7 2010	4.2	2.7/2.3
#8	14 2010	4.9	3.7/3.5
#9	17 2010	4.2	2.7/2.3
#10	25 2010	5	3.7/3.5

<sup>c</sup>Fit values when estimating 2000 accelerations per direction for the 2×2 gravity field model

<sup>d</sup>Fit values when estimating 1500 accelerations per direction for the 180×180 (full) gravity field model

Sect. "Solutions for the absorption of the contribution of the remaining dynamic models" (Table 1). The obtained results are included in Table 4. It is evident that the solutions based on the estimation of 1500 accelerations per direction have fits in the range from 4.2 to 5.0 mm. It follows that the RMS<sub>3D</sub> values for variants with the partial absorption of the gravity model are almost 2 mm greater than the corresponding values for the variants without the partial absorption of this model. This means a decrease in the efficiency of empirical accelerations after turning on the partial absorption of the gravity field model for the longer 1-day arcs. On the other hand, this absorption concerns a large part of the gravity model above the degree and order of 2 of spherical harmonic coefficients. However, in order to improve the fit of the estimated arcs, additional solutions were obtained for which the number of parameters determined was increased to 2,000 per direction. The results are presented in the last column of Table 4. They show a clear improvement over the results in column 3 of Table 4 and a reduction in the differences with the results, which do not take into account the absorption of the gravity model. The difference between the solutions with an increased number of estimated parameters and the results in Table 1 decreased from about 2.0 mm to about 0.2–0.4 mm. It is worth noting at this point once again that the obtained RMS<sub>3D</sub> values of the fits are, in all cases, with a large margin in the error of the reference orbit (~2 cm).

A separate issue when considering the longer 1-day arcs is the absorption of the entire gravity model with the exception of the main Newtonian term (keeping only the C<sub>00</sub>

coefficient). For all selected longer arcs, unlike the short 90-min arcs, no solution was reached due to a lack of convergence. It seems that, in such a case, the initial distance of the estimated orbit from the reference orbit at a level of about 20 km was too large to achieve the aforementioned convergence of solutions.

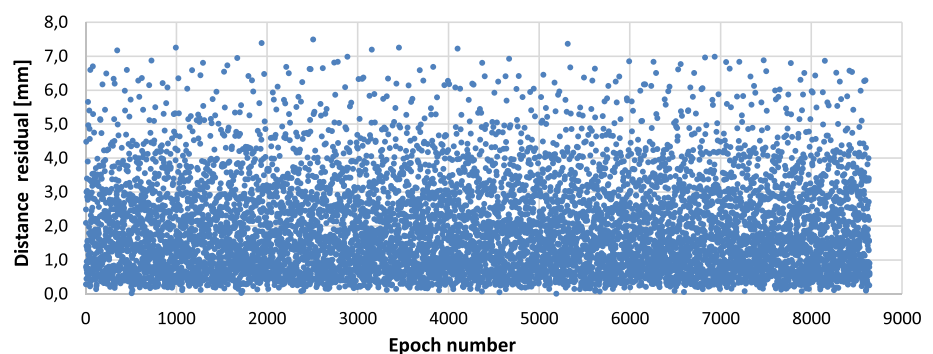
As for the 90-min arcs here are the results of determining the useful range of the gravity model for the two different 1-day orbit arcs. Table 5 contains the fits of the determined variants of the 1-day orbit arc #1 (2010, DOY: 311) for the selected gravity model truncation values and the corresponding  $RMS_a$  values of the estimated empirical accelerations. As can be seen, for the longer 1-day arc, the significant part of the gravity model reaches degree and order between 100 and 120 (an increase in  $RMS_a$  from  $2.45 \times 10^{-6} \text{ m/s}^2$  for degree and order at 120 to  $2.48 \times 10^{-6} \text{ m/s}^2$  for degree and order at 100). The closer inspection, with the determination of intermediate variants between the truncation values from 100 to 120, showed the significant part of the gravity model

**Table 5** Fits of the selected longer 1-day arc for the different degree and order of the gravity model truncation without using the remaining dynamic models. The case: 1500 estimated accelerations per each of the three directions

Truncation to degree and order	$RMS_{3D}$ (mm)	$RMS_a$ ( $\text{m/s}^2$ )
$180 \times 180^a$	2.3	$2.45 \times 10^{-6}$
$160 \times 160$	2.3	$2.45 \times 10^{-6}$
$140 \times 140$	2.3	$2.45 \times 10^{-6}$
$120 \times 120$	2.3	$2.45 \times 10^{-6}$
$100 \times 100$	2.3	$2.48 \times 10^{-6}$
$80 \times 80$	2.4	$2.70 \times 10^{-6}$
$60 \times 60$	2.6	$3.91 \times 10^{-6}$
$40 \times 40$	3.4	$9.18 \times 10^{-6}$
$20 \times 20$	4	$2.31 \times 10^{-5}$
$10 \times 10$	4.1	$3.92 \times 10^{-5}$
$5 \times 5$	4.2	$7.09 \times 10^{-5}$
$2 \times 2$	4.3	$1.24 \times 10^{-4}$
$2 \times 0$	4.3	$1.32 \times 10^{-4}$

<sup>a</sup>No truncation—the full gravity field model

**Fig. 1** The distance of the estimated orbit from the reference orbit for arc #1 ( $RMS_{3D} = 2.3 \text{ mm}$ )



up to degree and order 109. In turn, the analogous tests (not shown here) for the 1-day arc #10 (2010, DOY: 25) made it possible to determine the significant part of the gravity model up to degree and order of 112.

Comparing the determined values of degree and order of the gravity model truncation for the shorter 90-min and longer 1-day arcs, one can clearly see higher values for the latter arcs. In other words, the longer 1-day arcs show greater sensitivity to the gravity model than the shorter 90-min ones.

This may be related to a greater use of the gravity model for the longer 1-day arcs in the numerical integration process, which is an important part of the software used for the orbit estimation. By correlating the satellite's positions at successive epochs, of which there are many more for the 1-day arcs than for the 90-min arcs, the useful part of this model may be larger for the longer arcs.

## Analysis of the accuracy of the obtained results

As shown above, the results of fitting the estimated orbital arcs to the reference orbit are at the level of a few millimeters. In order to identify possible factors that may affect the obtained accuracy, additional tests were carried out. The results of these tests are presented in the following subsections.

### Fit accuracy analysis: distance residuals in the time domain and in the frequency domain

As can be seen from Table 1, three groups of solutions differing in the levels of  $RMS_{3D}$  values were obtained. Taking this into account, time series of distance residuals were determined for the longer 1-day arcs, covering the distances between the estimated orbit and the reference orbit at successive epochs. The following three figures show the time distributions of these residuals for three 1-day arcs belonging to each of the three aforementioned solution groups. These three arcs are representative for each group of solutions. From the first two figures (Figs. 1 and 2), it is clear that the

density of distance residuals increases as they approach zero, which suggests the normal distribution. In the case shown in Fig. 3 (arc #8), the residuals are arranged along two distinct bands. In the first band, the residuals concentrate around a value of about 2 mm, while in the second one around a value of about 7 mm. In other words, the residuals are clearly biased toward the two mentioned values. Moreover, the density of residuals in the band farther from zero is lower than for the band lying closer to zero. The observed distribution of residuals in this case demonstrates the imposition of pronounced systematic effects on the normal distribution. The very similar distribution of residuals was also obtained for arc #10.

To indicate the presence of periodic components, the time series of residuals were transformed into the frequency domain using the Fourier transform. Figure 4 presents the power spectral density (PSD) of the simulated time series of distance residuals with the normal distribution and standard deviation of 3.5 mm. This simulation was carried out using a normal distribution generator taken from (Press et al. 1992). By definition, with the strict normal distribution, there should be no periodic components associated with systematic effects. Thus, the peaks visible in Fig. 4 mark the level of numerical noise, which does not exceed 0.1 mm (Fig. 4). Figures 5, 6, 7 show the PSD of distance residuals for analogous representative arcs as in the case of the discussed Figs. 1, 2, 3. They show that the time series of distance

**Fig. 2** The distance of the estimated orbit from the reference orbit for arc #2 ( $RMS_{3D}=3.3$  mm)

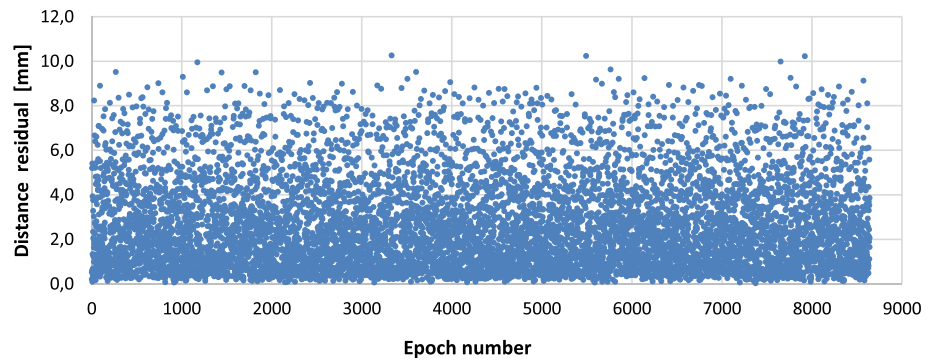


**Fig. 3** The distance of the estimated orbit from the reference orbit for arc #8 ( $RMS_{3D}=3.5$  mm)

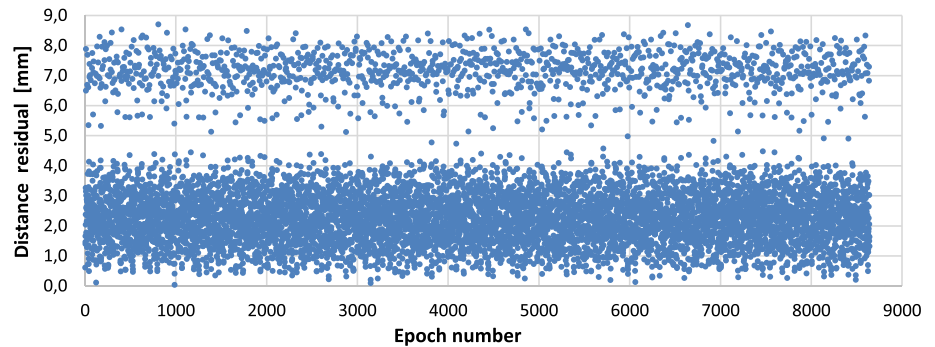


**Fig. 4** PSD of the simulated time series of distance residuals with the normal distribution and  $\sigma=3.5$  mm

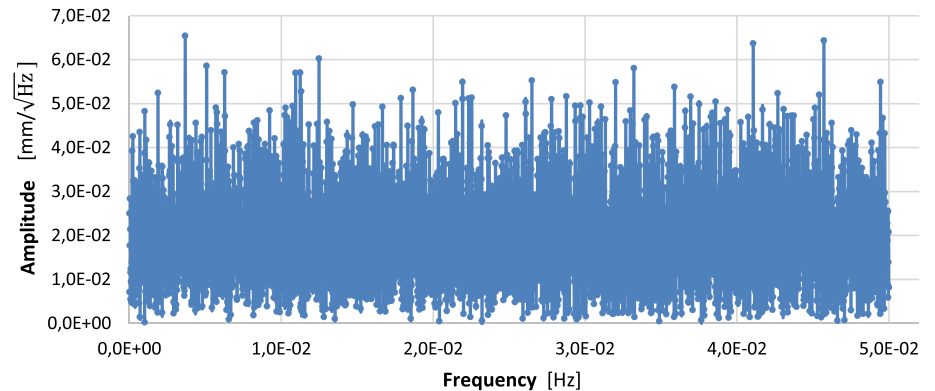




**Fig. 5** PSD of the time series of distance residuals for arc #1 ( $RMS_{3D} = 2.3$  mm)

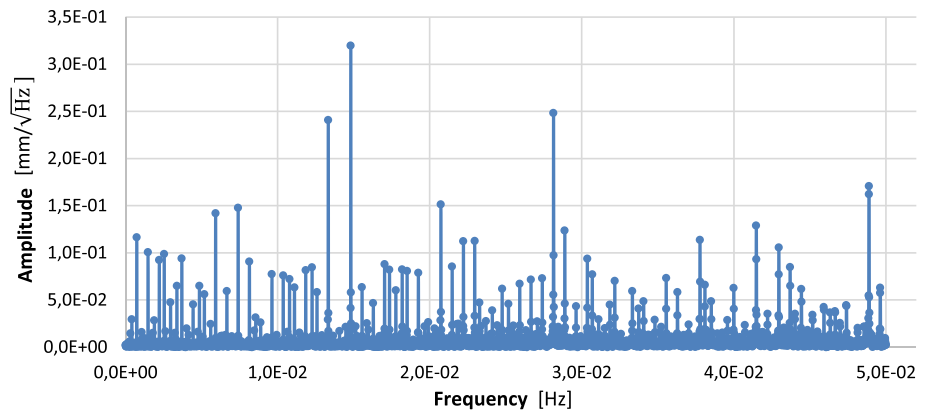


**Fig. 6** PSD of the time series of distance residuals for arc #2 ( $RMS_{3D} = 3.3$  mm)

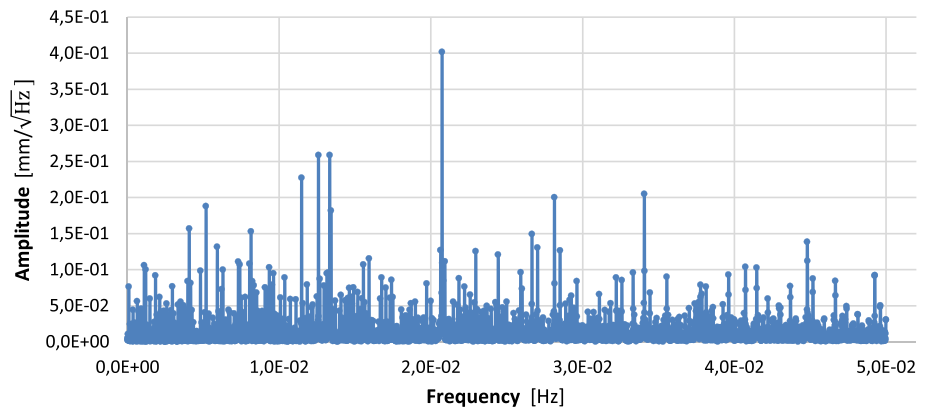
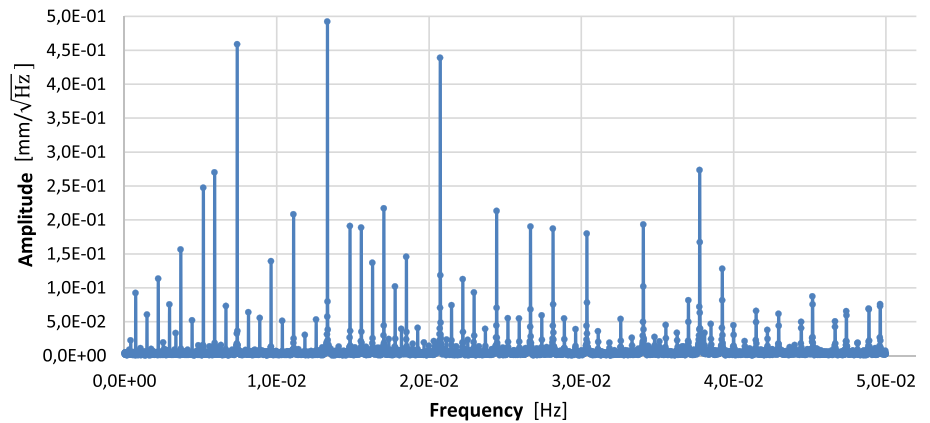


**Fig. 7** PSD of the time series of distance residuals for arc #8 ( $RMS_{3D} = 3.5$  mm)



residuals also contain systematic effects, i.e., periodic components with amplitudes reaching almost  $0.50$   $\text{mm}/\sqrt{\text{Hz}}$  (Fig. 7). The increase in  $RMS_{3D}$  for individual arcs from  $2.3$  mm through  $3.3$  to  $3.5$  mm corresponds to the increase in the level of amplitudes of systematic components seen in Figs. 5, 6, 7. The averages of the three largest components shown in Figs. 5, 6, 7 are:  $0.27$   $\text{mm}/\sqrt{\text{Hz}}$  (average for the three largest components in Fig. 5),  $0.31$   $\text{mm}/\sqrt{\text{Hz}}$  (average for the three largest components in Fig. 6) and  $0.46$   $\text{mm}/\sqrt{\text{Hz}}$  (average for the three largest components in Fig. 7). The periods of the aforementioned three largest components

(peaks) in Figs. 5, 6, 7 oscillate around the value of  $57.6$  s. with the exception of period of  $135.0$  s. for an amplitude of  $0.46$   $\text{mm}/\sqrt{\text{Hz}}$  in Fig. 7, which is about twice this value. The aforementioned value of  $57.6$  s. is the length of intervals at which constant empirical accelerations are determined in the orbit estimation process. Thus the systematic periodic components corresponding to the largest peaks in Figs. 5, 6, 7 can be related to the discretization error resulting from dividing the estimated arcs into the intervals of length of  $57.6$  s and determining discrete acceleration values within them.

Therefore, taking into account Figs. 1, 2, 3 and on the other hand Figs. 5, 6, 7, it can be noted that the distances of the estimated orbits from the reference orbits, described by the distance residuals, contain both a random component (Figs. 1, 2, 3) and systematic components (Figs. 3, 5, 6, 7).

### Fit accuracy analysis: estimating the effect of random errors of the reference orbit on the fit of selected arcs

Additional numerical tests were conducted to supplement the accuracy analysis presented in the previous section. They allowed to illustrate the sensitivity of the orbit fit process to selected values of random errors added to the rectangular coordinates of the reference orbit.

In order to present the effect of random errors of the reference orbit on the accuracy of the fit, the previously estimated orbits with the  $RMS_{3D}$  of 2.3 mm and of 3.5 mm were taken as the reference orbits. Thus, the fit without the modification of these orbits by random errors yields the  $RMS_{3D}$  value of 0.0 mm. The corresponding numerical tests were carried out for the arc #1–DOY: 311 2009 and #10–DOY: 25 2010. Both arcs occurred in two variants—the shorter arc with the length of 90 min and the longer one with the 1-day length. Random errors with the normal distribution (Press et al. 1992) for successive values of standard deviations were added to the Cartesian coordinates of the reference orbits prepared as described above. As can be clearly seen in Table 6, the standard deviations of the random errors added to the reference orbits are smaller than the corresponding  $RMS_{3D}$ . It is as if the mentioned standard deviations are amplified in the process of orbit determination. The increase in the  $RMS_{3D}$  values relative to the corresponding standard deviations is on average 23% (90-min arc #1) and 25% (90-min arc #10) as well as 57% (1-day arc #1) and 61% (1-day arc #10). These increases indicate that an accumulation of errors in the orbit determination process is taking place. This accumulation is greater for longer arcs. It can also be seen that the 1-day arc #10 with the larger primary  $RMS_{3D}$  value (3.5 mm, Table 1) has the larger percentage increase in the  $RMS_{3D}$  for the given standard deviation (61%) than the 1-day arc #1 with the smaller primary  $RMS_{3D}$  (2.3 mm, Table 1), where the corresponding increase is 57%. A part of this error accumulation is connected with a propagation of random errors to the  $RMS_{3D}$  value. This is caused by the fact that random errors with the given standard deviation were added to all three Cartesian coordinates of the satellite's position in the reference orbit. The aforementioned accumulation of errors may also be caused in part by the impact of the discretization error mentioned above (Sect. "Fit accuracy analysis: distance residuals in the time domain and in the frequency domain"). This error is related to the division of the orbital arc into a series of equal intervals at which empirical

**Table 6** Results of the fit for different values of standard deviations ( $\sigma$ ) of normal distribution random errors added to the reference orbits in the case of two selected arcs—each of them with the lengths: 90 min and 1-day. The number of estimated empirical accelerations: 269 per direction—for the shorter arc, 1500 per direction for the longer one

$\sigma$ (mm)	$RMS_{3D}$ (mm)			
	Arc #1– DOY: 90 min	311 2009 1-day	Arc #10– DOY: 90 min	25 2010 1-day
0	0	0	0	0
1	1.2	1.6	1.2	1.6
1.1	1.4	1.7	1.4	2.3
1.2	1.5	1.9	1.5	1.9
1.3	1.6	2	1.6	2.1
1.4	1.7	2.2	1.8	2.2
1.5	1.8	2.4	1.9	2.4
1.6	2	2.5	2	2.5
1.7	2.1	2.7	2.1	2.7
1.8	2.2	2.8	2.3	2.8
1.9	2.3	3	2.4	3
2	2.4	3.1	2.5	3.2
2.1	2.6	3.3	2.6	3.3
2.2	2.7	3.5	2.8	3.5
2.3	2.8	3.6	2.9	3.6
2.4	3	3.8	3	3.8
2.5	3.1	3.9	3.1	4
2.6	3.2	4.1	3.3	4.1
10	12.3	15.7	12.6	15.8

accelerations are estimated. With longer arcs, these intervals are more numerous, hence the cumulative effect is greater.

In Table 6 there are some specific values of standard deviations. With these values of standard deviations, the obtained  $RMS_{3D}$  values of the fit are close or equal to the ones obtained in the original orbit fit process (Table 1). This means that the level of the random component of the two tested reference orbits, expressed by the standard deviation of random errors with the normal distribution, is 1.4 mm and 2.3 mm (this value is the average of the two values for different lengths of arc #10, Table 6). It is worth noting the same (arc #1) or similar (arc #10–0.2 mm difference) values of these deviations for different arc lengths (in this case 90 min and 1 day). The larger standard deviation (2.3 mm) of the random component for the reference orbit arc #10 corresponds to the lower accuracy of the fit ( $RMS_{3D}$ : 3.0 mm and 3.5 mm for the 90-min and 1-day arc, respectively) compared to the arc #1 with the standard deviation of 1.4 mm ( $RMS_{3D}$ : 1.7 mm and 2.3 mm for the 90-min and 1-day arc, respectively).

### Fit accuracy analysis: estimating the impact of random errors of the gravity model on the fit of selected arcs

Taking into account the sensitivity of the fit accuracy of orbital arcs to random errors of the reference orbit, which was investigated earlier, a similar study was conducted for the gravity model used, in this case the gravity model Tongji-Grace02k (Chen et al. 2018). In order to determine the aforementioned effect of random errors of the gravity model on the accuracy of fitting the two selected orbit arcs, like in the previous chapter, in the first step for the reference orbit arcs #1 and #10, the corresponding fitted 1-day arcs were determined without modification of the gravity model. Then, in the second step, the two obtained (fitted) arcs were taken as the reference orbit arcs for subsequent computations. Thus, for the first variant of these computations without modifying the gravity model, the resulting  $RMS_{3D}$  values are close to zero. For the remaining variants, random errors were added to the coefficients (except for the  $C_{00}$  coefficient) of the gravity model. These errors forming a zero-mean Gaussian white noise with increasing values of standard deviations were obtained using the aforementioned random number generator (Press et al. 1992). The results are shown in Table 7. It can be clearly seen that for both arcs the modification of gravity field coefficients by adding random errors with the standard deviation up to  $10^{-11}$  does not significantly change the  $RMS_{3D}$  values. These values are close to zero at a level of  $10^{-2}$ – $10^{-3}$  mm with constant the  $RMS_a$  values of the estimated empirical accelerations. The addition of random errors with the standard deviation of  $10^{-10}$  causes a significant increase in the  $RMS_{3D}$  value to a level of about  $10^{-1}$  mm. At the same time, the  $RMS_a$  values are also

increasing from  $2.45$  to  $2.48 \times 10^{-6}$   $m/s^2$  (arc #1) and from  $9.33 \times 10^{-7}$   $m/s^2$  to  $1.01 \times 10^{-6}$   $m/s^2$  (arc #10). Interestingly, a further increase in the  $\sigma$  value by successive orders of magnitude up to  $10^{-6}$  results in corresponding increases in the  $RMS_{3D}$  of fit and  $RMS_a$  values in both cases almost exactly every one order of magnitude as well. In the extreme case, a reduction in the fit accuracy for the  $\sigma$  value of  $10^{-6}$  for both tested arcs means an increase in the  $RMS_{3D}$  value almost to the level of one meter and in the  $RMS_a$  value to the level of  $10^{-3}$   $m/s^2$ . Looking at the results in Table 7, it is clear that the  $\sigma$  value of  $10^{-10}$  is the threshold of sensitivity of the orbit determination process to random errors of the gravity field model. On the other hand, analyzing the values of the formal errors of the coefficients of the Tongji-Grace02k model used, it can be seen that the values of these errors at the level of  $10^{-10}$  appear for coefficients of degree of 146 and of order of 144 and above. It is known from other numerical tests that this range of coefficients does not have a significant impact on the orbit of the satellite. Taking into account the results from Table 7, it can be concluded that the contribution of random errors of the gravity model used to the overall error budget of the orbit fit does not exceed 0.1 mm.

In order to show the impact of using different gravity field models on the orbit fit, appropriate numerical tests were carried out by taking 13 models from different years. These models, like the aforementioned Tongji-Grace02k model, were taken from the International Centre for Global Earth Models (ICGEM) (Ince et al. 2019). The same 1-day arcs as above were selected for the orbit fit process. In each case, the same number of 4500 empirical accelerations was estimated. The results obtained show the error absorption of the different gravity models by the sets of estimated empirical accelerations (Table 8). For both arcs, one can see the better performance of the group of gravity models released after the year 2000 compared to older models; a systematic increase in fitting accuracy is observed when going from older to newer models. Characteristically, the larger the  $RMS_{3D}$  of the fit, the larger the  $RMS_a$  values of the empirical accelerations are at the same time. The aforementioned systematic increase in fitting accuracy stops at the EGM96 model-subsequent models give the same  $RMS_{3D}$  values- 2.3 mm for the first and 3.5 mm for the second arc.

Also, the  $RMS_a$  values of the estimated accelerations are practically at the same level. This means that the performance of newer models in the studied aspect of orbit determination with estimation of empirical accelerations does not show significant differences. As shown by the analysis of the values of the formal errors of the coefficients of the gravity models used, the obtained fitting results reflect their different levels. More strictly speaking, dominant formal errors of the coefficients of the long-term part of the selected gravity models are at the level of  $10^{-10}$  and above for the gravity models prior to the year 2000. For the gravity

**Table 7** Fits for different values of standard deviations ( $\sigma$ ) of normal distribution random errors added to the coefficients of gravity model in the case of the two selected 1-day arcs. The number of estimated empirical accelerations: 1500 per direction

$\sigma$	$RMS_{3D}(\text{mm})/RMS_a (m/s^2)$	
	Arc #1 DOY: 311 2009	Arc #10 DOY: 25 2010
0	$2.1 \times 10^{-3}/2.45 \times 10^{-6}$	$1.8 \times 10^{-3}/9.33 \times 10^{-7}$
$10^{-15}$	$1.6 \times 10^{-2}/2.45 \times 10^{-6}$	$4.7 \times 10^{-3}/9.33 \times 10^{-7}$
$10^{-14}$	$7.6 \times 10^{-3}/2.45 \times 10^{-6}$	$9.2 \times 10^{-3}/9.33 \times 10^{-7}$
$10^{-13}$	$5.0 \times 10^{-3}/2.45 \times 10^{-6}$	$4.8 \times 10^{-3}/9.33 \times 10^{-7}$
$10^{-12}$	$1.5 \times 10^{-3}/2.45 \times 10^{-6}$	$1.8 \times 10^{-3}/9.33 \times 10^{-7}$
$10^{-11}$	$1.6 \times 10^{-2}/2.45 \times 10^{-6}$	$9.2 \times 10^{-3}/9.33 \times 10^{-7}$
$10^{-10}$	$9.0 \times 10^{-2}/2.48 \times 10^{-6}$	$8.9 \times 10^{-2}/1.01 \times 10^{-6}$
$10^{-09}$	$9.0 \times 10^{-1}/4.65 \times 10^{-6}$	$9.0 \times 10^{-1}/4.04 \times 10^{-6}$
$10^{-08}$	$8.9 \times 10^0/3.95 \times 10^{-5}$	$8.9 \times 10^0/3.94 \times 10^{-5}$
$10^{-07}$	$8.9 \times 10^1/3.94 \times 10^{-4}$	$8.9 \times 10^1/3.94 \times 10^{-4}$
$10^{-06}$	$8.9 \times 10^2/3.94 \times 10^{-3}$	$8.9 \times 10^2/3.94 \times 10^{-3}$

**Table 8**  $RMS_{3D}$  values of the fit of selected 1-day arcs and corresponding  $RMS_a$  values of empirical accelerations depending on the adopted gravity model for 1500 estimated accelerations per each of the three directions

Gravity model	References	$RMS_{3D}(\text{mm})/RMS_a (\text{m/s}^2)$	
		Arc #1 DOY: 311 2009	Arc #10DOY: 25 2010
SE1	Lundquist et al. (1966)	4.2/6.33 × 10 <sup>-5</sup>	4.9 / 6.36 × 10 <sup>-5</sup>
GEM1	Lerch et al. (1972)	4.1/3.91 × 10 <sup>-5</sup>	4.8 / 3.95 × 10 <sup>-5</sup>
GEM10	Lerch et al. (1979)	4.0/2.56 × 10 <sup>-5</sup>	4.7 / 2.63 × 10 <sup>-5</sup>
GRIM4c1	Schwintzer et al. (1991)	3.3/1.37 × 10 <sup>-5</sup>	4.2 / 1.35 × 10 <sup>-5</sup>
OSU91a	Rapp et al. (1991)	2.7/9.53 × 10 <sup>-6</sup>	3.8 / 9.53 × 10 <sup>-6</sup>
JGM3	Tapley et al. (1996)	2.7/6.81 × 10 <sup>-6</sup>	3.8 / 6.49 × 10 <sup>-6</sup>
EGM96	Lemoine et al. (1998)	2.5/4.58 × 10 <sup>-6</sup>	3.6 / 9.29 × 10 <sup>-7</sup>
EGM2008	Pavlis et al. (2012)	2.3/2.45 × 10 <sup>-6</sup>	3.5 / 9.30 × 10 <sup>-7</sup>
GOCO02s	Goiginger et al. (2011)	2.3/2.45 × 10 <sup>-6</sup>	3.5 / 9.30 × 10 <sup>-7</sup>
GO_CONS_GCF_ _2_TIM_R4	Pail et al. (2011)	2.3/2.45 × 10 <sup>-6</sup>	3.5 / 9.33 × 10 <sup>-7</sup>
ITSG-Grace2014s	Mayer-Gürr et al. (2014)	2.3/2.45 × 10 <sup>-6</sup>	3.5 / 9.33 × 10 <sup>-7</sup>
ITSG-Grace2018s	Kvas et al. (2019)	2.3/2.45 × 10 <sup>-6</sup>	3.5 / 9.33 × 10 <sup>-7</sup>
Tongji-GMMG2021S	Chen et al. (2022)	2.3/2.45 × 10 <sup>-6</sup>	3.5 / 9.33 × 10 <sup>-7</sup>

models released after the year 2000, they are several orders of magnitude smaller falling even to  $10^{-14}$ . It should be noted that the deterioration of fit to the  $RMS_{3D}$  of 2.5 mm occurs when using the EGM96 model. For this model, the formal errors of the coefficients of the long-wave and mid-wave parts reach the level of  $10^{-10}$ . This would indicate the aforementioned threshold (just  $10^{-10}$ ) of sensitivity of the orbit determination process to random errors of the gravity field model coefficients. Near this value, there is a significant increase in the obtained  $RMS_{3D}$  value.

## Summary and conclusions

The selected orbital arcs of an example of low-Earth-orbiting satellite, in this case the GOCE satellite, were estimated by fitting to the appropriate reference arcs in the least-squares sense by correcting the initial conditions and determining sets of empirical accelerations. The performed numerical tests showed the possibility of absorbing the contribution of dynamic models, i.e., absorption of the contribution of a part of the gravity model above the degree and order of two of its coefficients and the absorption of the entire contribution of the remaining dynamic models. Moreover, because of the efficiency of the estimated empirical accelerations, the same millimeter-level of fit of the estimated orbits was achieved both with and without the use of dynamic models, i.e., the part of gravity model and the remaining dynamic models, which illustrates the aforementioned possibility of omitting the mentioned models in the process of estimating the orbit of the given satellite. Taking into account the aforementioned millimeter-level of obtained fits and the centimeter-level accuracy of the reference orbit, it can be

concluded that the accuracy of the determined orbits remains at the level of the reference orbit accuracy.

It should be clearly emphasized that the numerical tests carried out indicate, the effectiveness and usefulness of empirical accelerations in the orbit estimation process for an extremely low satellite (average altitude of about 250 km) such as the GOCE satellite. The results obtained, as already mentioned, place the determined orbit at the level of accuracy of the reference orbit. However, it is necessary to take into account, in addition to empirical accelerations, at least the truncated gravity model and simultaneous estimation of corrections to the initial conditions. Obtaining equivalent accuracy of the estimated orbits with and without the dynamic models points out the computational option of omitting them in the orbit determination process. This option of determining the orbit in the case under study with the omission of part of the gravity field model and other dynamic models can be considered in a cognitive aspect. Practically, it means the simplification of the mathematical model used in the orbit estimation process.

In order for the empirically estimated accelerations to effectively replace the aforementioned models, it is necessary for the orbit determination process to have a set of observations that are as accurate as possible. Then the orbit determination process has a fitting aspect. As the studies in (Novak et al. 2023) show, for example, when predicting the orbits of Global Navigation Satellite System satellites, dynamic models play a leading role. However, in such the case the empirical accelerations can cause deterioration of prediction results.

The aforementioned possibility that the dynamic models could be omitted from the orbit determination process may be due to the adoption in this work of pseudo-observations, which were the Cartesian coordinates of the reference orbit,

which are admittedly functions of real observations, but in a processed and refined form. In the general case, the orbit determination is a process in which there is a balance between the strength of dynamic models and the strength of observations. On the other hand, the estimation of additional empirical accelerations could compensate for imperfections in the dynamic models. In order to assess to what extent the omission of dynamic models in the orbit determination is significant relative to the option of keeping them, when estimating empirical accelerations in both cases, additional comparative tests with other sets of observations are necessary. Such tests are planned in the future using sets of simulated distance measurements between a low-Earth orbit satellite and the Global Positioning System satellites.

The obtained values of the fits at the level of a few millimeters were the starting point for an analysis of factors, which may influence this accuracy. The time series of distance of the estimated orbit from the reference orbit in the time and frequency domain made it possible to indicate the occurrence of errors of both random and systematic character. Additional tests were also carried out, in which in the first variant random errors of different standard deviations were added to a properly prepared reference orbit, and in the second one the coefficients of the gravity field model were modified with these errors. The obtained results show that the dominant factor in the accuracy of fits is connected with random errors of the reference orbit. Caused by them, the value of contribution to the obtained values of fits, given by the  $RMS_{3D}$  values, reaches more than 2 mm. In turn, the value of contribution caused by the aforementioned systematic errors generated by dividing the estimated arcs into equal intervals in which the acceleration values are estimated (discretization error) reaches a few tenths of a millimeter. Finally, the contribution from random errors of the gravity field model does not exceed 0.1 mm, provided that the newer gravity model, issued after 2000, is used. As additional tests have shown, the use of older models, prior to 2000, causes a significant increase in the fitting error. This increase can reach up to 2 mm.

Taking into account the fit level of the obtained orbital arcs, it is also possible to indicate the potential possibility of the presented fit process for interpolation of the reference orbits. This implies the adoption in this process of an integration step smaller than the sampling interval of these orbits, which also took place in the research carried out as part of this study.

## Declarations

**Conflict of interest** On behalf of all authors, the corresponding author states that there is no conflict of interest.

**Open Access** This article is licensed under a Creative Commons Attribution 4.0 International License, which permits use, sharing,

adaptation, distribution and reproduction in any medium or format, as long as you give appropriate credit to the original author(s) and the source, provide a link to the Creative Commons licence, and indicate if changes were made. The images or other third party material in this article are included in the article's Creative Commons licence, unless indicated otherwise in a credit line to the material. If material is not included in the article's Creative Commons licence and your intended use is not permitted by statutory regulation or exceeds the permitted use, you will need to obtain permission directly from the copyright holder. To view a copy of this licence, visit <http://creativecommons.org/licenses/by/4.0/>.

## References

- Bobojć A, Drozyner A (2011) GOCE satellite orbit in aspect of selected gravitational perturbations. *Acta Geophys* 59(2):428–452. <https://doi.org/10.2478/s11600-010-0052-3>
- Bock H, Jäggi A, Meyer U, Visser P, Van den Ijssel J, Van Helleputte T, Heinze M, Hugentobler U (2011) GPS-derived orbits for the GOCE satellite. *J Geodesy* 85(11):807–818. <https://doi.org/10.1007/s00190-011-0484-9>
- Bock H, Jäggi A, Beutler G, Meyer U (2014) GOCE: precise orbit determination for the entire mission. *J Geodesy* 88(11):1047–1060. <https://doi.org/10.1007/s00190-014-0742-8>
- Chen Q, Shen Y, Francis O, Chen W, Zhang X, Hsu H (2018) Tongji-Grace02s and Tongji-Grace02k: high-precision static GRACE-Only global earth's gravity field models derived by refined data processing strategies. *J Geophys Res: Solid Earth* 123(7):6111–6137. <https://doi.org/10.1029/2018JB015641>
- Chen J, Zhang X, Chen Q, Shen Y, Nie Y (2022) Static gravity field recovery and accuracy analysis based on reprocessed GOCE level 1b gravity gradient observations, EGU general assembly 2022, Vienna, Austria, 23–27 May 2022, EGU22-6771. <https://doi.org/10.5194/egusphere-egu22-6771>
- Drinkwater M, Floberghagen R, Haagmans R, Muzi D, Popescu A (2003) GOCE: ESA's first earth explorer core mission. *Space Sci Rev* 108:419–432. <https://doi.org/10.1023/A:1026104216284>
- Drozyner A (1995) Determination of orbits with Toruń orbit processor system. *Adv Space Res* 16(12):93–95. [https://doi.org/10.1016/0273-1177\(95\)98788-P](https://doi.org/10.1016/0273-1177(95)98788-P)
- ESA (2010) GOCE level 2 product data handbook. European GOCE Gravity Consortium. ESA Tech. Note GO-MA-HPF-GS-0110, European Space Agency, Noordwijk
- Goiginger H, Höck E, Rieser D, Mayer-Guerr T, Maier A, Krauss S, Pail R, Fecher T, Gruber T, Brockmann J, Krasbutter I, Schuh W, Jaeggi A, Prange L, Hausleitner W, Baur O, Kusche J (2011) The combined satellite-only global gravity field model GOCO02S—presented at the 2011 General Assembly of the European Geosciences Union, Vienna, Austria, April 4–8
- Ince E, Barthelmes F, Reißland S, Elger K, Förste C, Flechtner F, Schuh H (2019) ICGEM—15 years of successful collection and distribution of global gravitational models, associated services, and future plans. *Earth Syst Sci Data* 11:647–674. <https://doi.org/10.5194/essd-11-647-2019>
- Jäggi A, Hugentobler U, Beutler G (2006) Pseudo-stochastic orbit modeling of low earth satellites using the global positioning system. *J Geod* 80:47–60. <https://doi.org/10.1007/s00190-006-0029-9>
- Jäggi A, Hugentobler U, Bock H, Beutler G (2007) Precise orbit determination for GRACE using undifferenced or doubly differenced GPS data. *Adv Space Res* 39:1612–1619. <https://doi.org/10.1016/j.asr.2007.03.012>

- Kang Z, Nagel P, Pastor R (2003) Precise orbit determination for GRACE. *Adv Space Res* 31(8):1875–1881. [https://doi.org/10.1016/S0273-1177\(03\)00159-5](https://doi.org/10.1016/S0273-1177(03)00159-5)
- Kang Z, Bettadpur S, Nagel P, Save H, Poole S, Pie N (2020) GRACE-FO precise orbit determination and gravity recovery. *J Geodesy* 94:85. <https://doi.org/10.1007/s00190-020-01414-3>
- Kvas A, Behzadpour S, Ellmer M, Klinger B, Strasser S, Zehentner N, Mayer-Gürr T (2019) ITSG-Grace2018: overview and evaluation of a new GRACE-only gravity field time series. *J Geophys Research: Solid Earth* 124(8):7519–9453. <https://doi.org/10.1029/2019JB017415>
- Lemoine F, Kenyon S, Factor J, Trimmer R, Pavlis N, Chinn D, Cox C, Klosko S, Luthcke S, Torrence M, Wang Y, Williamson R, Pavlis E, Rapp R, Olson T (1998) The development of the joint NASA GSFC and the National Imagery and Mapping Agency (NIMA) Geopotential Model EGM96; NASA Technical Paper NASA/TP1998206861, Goddard Space Flight Center, Greenbelt, USA
- Lerch F, Wagner C, Smith D, Sandson M, Brown J, Richardson J (1972) Gravitational field models for the earth (GEM1&2); Report X55372146, Goddard Space Flight Center, Greenbelt/Maryland
- Lerch F, Klosko S, Laubscher R, Wagner C (1979) Gravity Model Improvement Using Geos3 (GEM9 and 10). *J Geophys Res* 84(B8):3897–3916
- Lundquist C, Veis G (1966) Geodetic Parameters for a 1966 Smithsonian Institution Standard Earth; Special Report No. 200, Smithsonian Astrophysical Observatory, Cambridge/Mass
- Mao X, Arnold D, Girardin V, Villiger A, Jäggi A (2021) Dynamic GPS-based LEO orbit determination with 1 cm precision using the Bernese GNSS software. *Adv Space Res* 67(2):788–805. <https://doi.org/10.1016/j.asr.2020.10.012>
- Mayer-Gürr T, Kurtenbach E, Eicker A (2010) ITG-Grace2010: the new GRACE gravity field release computed in Bonn. *Geophys Res Abstr* 12:2446
- Mayer-Gürr T, Zehentner N, Klinger B, Kvas A (2014) ITSG-Grace2014: a new GRACE gravity field release computed in Graz. GRACE Science Team Meeting 2014, Potsdam
- Moore P, Wang J (2005) On reduced dynamic orbits for altimetric satellites. *Adv Space Res* 36(3):445–453. <https://doi.org/10.1016/j.asr.2005.04.059>
- Novak A, Zajdel R, Sošnica K (2023) Optimization of orbit prediction strategies for GNSS satellites. *Acta Astronaut* 209:132–145. <https://doi.org/10.1016/j.actaastro.2023.04.040>
- Pail R, Bruinsma S, Migliaccio F, Foerste C, Goiginger H, Schuh W, Hoek E, Reguzzoni M, Brockmann J, Abrikosov O, Veicherts M, Fecher T, Mayrhofer R, Krasbutter I, Sanso F, Tscherning C (2011) First GOCE gravity field models derived by three different approaches. *J Geodesy* 81:11. <https://doi.org/10.1007/s00190-011-0467-x>
- Pavlis K, Holmes S, Kenyon S, Factor J (2012) The development and evaluation of the earth gravitational model 2008 (EGM2008). *J Geophys Res: Solid Earth* 117:B04406. <https://doi.org/10.1029/2011JB008916>
- Press W, Teukolsky S, Vetterling W, Flannery B (1992) Numerical recipes in FORTRAN, 2nd edn. University Press, Cambridge
- Rapp R, Wang Y, Pavlis K (1991) The Ohio state 1991 geopotential and sea surface topography harmonic coefficient models; The Ohio State University, Department of Geodetic Science, Report No. 410, Columbus/Ohio
- Reigber Ch, Jochmann H, Wunsch J, Petrovic S, Schwitzer P, Barthelmes F, Neumayer KH, König R, Förste Ch, Balmino G, Biancale R, Lemoine JM, Loyer S, Perosanz F (2005) Earth gravity field and seasonal variability from CHAMP. Earth observation with CHAMP—results from 3 years in orbit. Springer, Berlin, pp 25–30
- Rummel R, Yi W, Stummer C (2011) GOCE Gravitational Gradiometry. *J Geod* 85:777–790. <https://doi.org/10.1007/s00190-011-0500-0>
- Schwintzer P, Reigber Ch, Massmann F, Barth W, Raimondo J, Gerstl M, Li H, Biancale R, Balmino G, Moynot B, Lemoine J, Marty J, Boudon Y, Barlier F (1991) A new earth gravity field model in support of ERS-1 and SPOT-2; Final Report to the German Space Agency (DARA) and the French Space Agency (CNES); DGFI München, GRGS Toulouse
- Tapley B, Watkins M, Ries J, Davis G, Eanes R, Poole S, Rim H, Schutz B, Shum C, Nerem R, Lerch F, Marshall J, Klosko S, Pavlis N, Williamson R (1996) The Joint Gravity Model 3. *J Geophys Res* 101(B12):28029–28049
- Tapley B, Bettadpur S, Watkins M, Reigber C (2004) The gravity recovery and climate experiment: mission overview and early results. *Geophys Res Lett* 31(9):4. <https://doi.org/10.1029/2004GL019920>
- Wang Z, Li Z, Wang L, Wang N, Yang Y, Li R, Zhang Y, Liu A, Yuan H, Hoque M (2022) Comparison of the real-time precise orbit determination for LEO between kinematic and reduced-dynamic modes. *Measurement*. <https://doi.org/10.1016/j.measurement.2021.110224>